Available online at www.sciencedirect.com
ScienceDirect
Journal of the European Ceramic Society 28 (2008) 577–584
www.elsevier.com/locate/jeurceramsoc

The effect of the valence state of titanium ions on the hydrophilicity of ceramics in the titanium–oxygen system

Danjela Kuscer [a,*], Janez Kovač [a], Marija Kosec [a], Ronn Andriesen [b]

[a] *Jozef Stefan Institute, Jamova 39, SI-1000 Ljubljana, Slovenia*
[b] *Agfa-Gevaert, Septestraat 27, B-2640 Mortsel, Belgium*

Received 22 March 2007; received in revised form 2 July 2007; accepted 6 July 2007
Available online 21 September 2007

Abstract

Ceramics from the titanium–oxygen system were prepared by sintering TiO_2 and Ti_2O_3 powders at 1400 °C in air or in Ar/H_2 (7%). The surface compositions of the TiO_2, the non-stoichiometric TiO_{2-x} and the Ti_2O_3 ceramics, studied with X-ray photoelectron spectroscopy, are discussed in terms of their chemical composition, with particular emphasis on the valence state of the titanium ions. The correlation between the valence state of the titanium ions at the surface and the water-contact angle was examined. The presence of Ti^{3+}, which can be introduced at the titanium–oxygen ceramic surface by sintering the ceramic in lower oxygen partial pressure, is related to a significant decrease in the water-contact angle. TiO_2 ceramics with just Ti^{4+} at the interface had a water-contact angle of 67°; however, the non-stoichiometric TiO_{2-x} and Ti_2O_3/Ti_3O_5 with Ti^{3+} at the interface had lower water-contact angles, i.e., 26° and 18°, respectively. The wettability of ceramics in the Ti–O system can be improved by introducing Ti^{3+} at the ceramic interface.

Keywords: Sintering; Defects; Surfaces; TiO_2; Sensors; Wetting

1. Introduction

TiO_2 attracts particular interest because of two photo-induced phenomena, i.e., the photocatalytic and superhydrophilic effects.[1–4] TiO_2 has the ability to decompose many organic compounds due to the photocatalytic effect, a phenomenon that has been studied extensively.[5–7] When TiO_2 is illuminated with photons whose energy is equal to or greater than the TiO_2 band-gap energy, E_g, these photons are absorbed, and as a consequence electron–hole pairs are created. The electron–hole pairs further dissociate into free photoelectrons in the conduction band and photo-holes in the valence band. These photo-generated carriers can react with oxygen and water from the surroundings to produce the radicals $^{\bullet}O_2^-$ and $^{\bullet}OH^-$ that can recombine and decompose organic compounds.[4,6,7]

The second phenomenon, superhydrophilicity has been observed in TiO_2. When TiO_2 is illuminated with light of a specific wavelength, the surface becomes more hydrophilic, i.e., the water-contact angle decreases. Previous reports suggest that the super-hydrophilicity of TiO_2 after UV illumination is related to the reduction of Ti^{4+} to the Ti^{3+} state.[4,5] The electron that is formed under UV illumination tends to reduce the Ti^{4+} cations to the Ti^{3+} state and consequently oxygen vacancies are created. Water molecules can then occupy the oxygen vacancies, producing chemisorbed –OH groups, which increases the Van der Waals forces and the hydrogen-bonding interactions between the H_2O and the –OH, and as a result of this the hydrophilic properties are enhanced.[4,5] Fujishima et al.[4] reported that the water-contact angle of a TiO_2 anatase thin film is 15°, and that the angle decreases significantly after UV illumination. The water spreads over the anatase surface and the contact angle was estimated to be close to 0°. However, this increased hydrophilicity was not permanent and after a few hours in the dark the TiO_2 reverts to its more hydrophobic state.[4] For practical applications it is highly desirable that the surface of TiO_2 exhibits a high wettability with respect to water in addition to a photocatalytic effect. Such a surface ensures that surface contaminants are either photo-mineralised or washed away by water.

Titanium dioxide exists in three crystal structures,[8] i.e., rutile, brookite and anatase. When brookite and anatase are heated

* Corresponding author. Tel.: +386 1477 3489; fax: +386 1477 3887.
E-mail address: danjela.kuscer@ijs.si (D. Kuscer).

0955-2219/$ – see front matter © 2007 Elsevier Ltd. All rights reserved.
doi:10.1016/j.jeurceramsoc.2007.07.014

to temperatures between 700 and 920 °C they transform irreversibly to rutile.[9] Rutile crystallizes in a tetragonal structure with $a = 0.4594(3)$ nm and $c = 0.2959(3)$ nm.[10] Its properties are determined by the non-stoichiometry and the concentrations of various defects that can exist in the TiO_2 lattice. In addition, the properties of the TiO_2 surface can be greatly affected by the bulk structure and defects, as has been extensively reviewed.[11]

In addition to stoichiometric TiO_2, a lot of work has been done on non-stoichiometric TiO_{2-x}. The degree of non-stoichiometry significantly depends on the temperature and the oxygen partial pressure, as has been thoroughly reviewed.[12] Ti interstitials are regarded as the major defects at high temperatures.[13] The non-stoichiometry parameter x in TiO_{2-x} increases with increasing temperature and is reported to have an upper limit in air of 0.008 at 1000 °C and 0.016 at 1400 °C.[12]

For larger deviations from the TiO_2 stoichiometry, the oxide forms a series of compounds with ordered structures that appear between the non-stoichiometric TiO_{2-x} and Ti_2O_3. These structures are known as Magnéli phases,[14] and have the composition Ti_nO_{2n-1}, where $3 \leq n \leq 20$. Ti_2O_3 is isostructural with Al_2O_3, having the rhombohedral unit-cell dimensions $a = 0.54325(8)$ nm and $\alpha = 56.75(1)°$.[15] A phase diagram indicating all the compounds between Ti_2O_3 and TiO_2 is shown in Fig. 1.

There is a growing interest in understanding and possibly controlling the surface properties of TiO_2. Earlier investigations showed that the (1 1 0) surface possesses the lowest energy,[16] and for this reason it has been the most extensively studied. It was also confirmed that the hydrophilic-to-hydrophobic conversion of the TiO_2 surface can be induced by irradiating the sample with light of a specific wavelength.[17,18] However, the results concerning the contact angle of water on non-irradiated TiO_2 surfaces are rather inconsistent, with the angle ranging from 72°[18] to less than 10°.[19] There are numerous factors that can have an effect on the water-contact angle. For example, it is well known that atmospheric contaminants accumulate on a TiO_2 surface,[20] and as a consequence the contact angle increases. The surface roughness is also known to play an important role in influencing the water-contact angle.[17] Since the TiO_2 surface is hydrophilic, i.e., the reported contact angles are less than 90°, the lower contact angle may be the result of surface roughness. To the best of our knowledge even less information is available on the wettability of non-stoichiometric titanium oxide and Ti_nO_{2n-1} than for TiO_2.

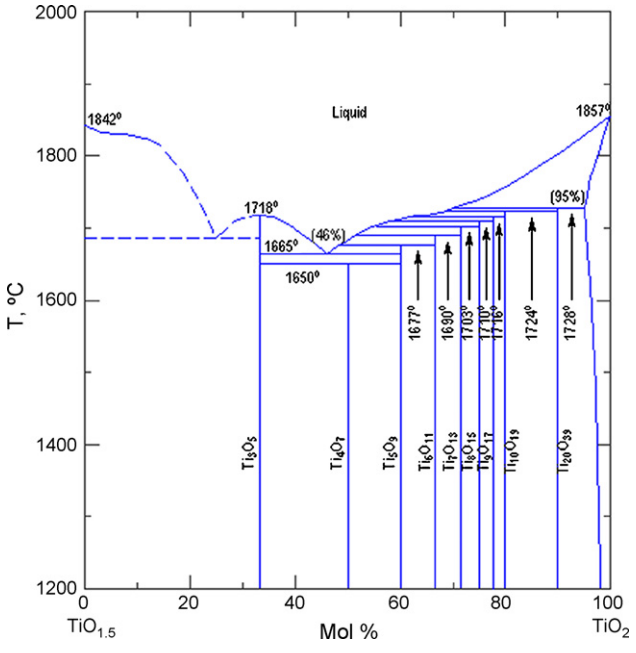

Fig. 1. Phase diagram of $TiO_{1.5}$–TiO_2.

The motivation for the present investigations was to find an alternative method, i.e., other than UV illumination, for enhancing the wettability of ceramics in the Ti–O system. Bulk TiO_2, non-stoichiometric TiO_{2-x} and Ti_2O_3 ceramics were prepared by sintering TiO_2 and Ti_2O_3 at various oxygen partial pressures, and the chemical compositions of their surfaces were investigated. The contact angle of water on the Ti–O ceramic surfaces is reported and correlated to the surface composition of the TiO_2, the non-stoichiometric TiO_{2-x} and the Ti_2O_3.

2. Experimental

For the experimental work we used commercially available TiO_2 (99.9%) and Ti_2O_3 (99.8%) powders, both from Alfa Aesar, Karlsruhe, Germany.

The non-stoichiometric TiO_2 powder (denoted TiO_{2-x}) was prepared from stoichiometric TiO_2 powder by heating it at 1400 °C for 2 h in Ar/H_2 (7%). After the heating, the powder had a dark colouration.

The Ti_2O_3 powder was high-energy milled in a planetary mill (Retsch, Model PM 400, Hann, Germany). A 250-ml tungsten carbide (WC) milling jar filled with 15 tungsten carbide balls of 20-mm diameter was used. A total of 200 g of powder was placed in the vial. The rotational speed of the supporting disk was set to 300 rpm. The milling conditions are detailed in reference.[21]

The TiO_2 ceramic was prepared from TiO_2 powder by sintering in air; the non-stoichiometric TiO_{2-x} ceramic was prepared from TiO_{2-x} powder by sintering in Ar/H_2 (7%); and the Ti_2O_3 ceramic was prepared from mechano-chemically activated Ti_2O_3 powder by sintering in Ar/H_2 (7%). All the powders were sintered at 1400 °C for 2 h.

During the thermal treatment of the TiO_{2-x} and Ti_2O_3 in Ar/H_2 (7%), titanium sponges were placed ahead of and behind the sample in the furnace to trap the impurities and ensure that only uncontaminated Ar/H_2 (7%) reached the sample. The furnace tube was used exclusively for thermally treating Ti–O ceramics and so any contamination from earlier firings is ruled out. The oxygen partial pressure in Ar/H_2 (7%) was measured using a Rapido 3100 Oxygen Analyser (Cambridge Sensotec Ltd., Cambridge, UK). The amount of oxygen in the gas before entering the tube furnace was 10^{-19} ppm at room temperature and at the exit of the tube furnace where the temperature was between 400 and 500 °C it was 10^{-17} ppm.

X-ray powder-diffraction data were collected from the samples at room temperature on an Endeavor Bruker AXS, Model D4 (Karlsruhe, Germany) diffractometer using Cu Kα radiation. The data were collected in the 2θ range from 20° to 70° in steps

of 0.02°, with an integration time of 4 s per step. The peak positions and the relative heights of the peaks were determined from the experimental patterns after filtering out the Cu $K\alpha_2$ radiation component. The observed phases were identified using the PDF-2[22] database.

The sintering curves of the powder were recorded with a heating-stage microscope (Leitz Wetzlar, Germany) in the temperature range 25–1350 °C at a heating rate of 10 °C/min in air and in Ar/H_2 (7%).

The thermal analysis (Thermogravimetry TG, Netzsch STA 409, Selb, Germany) was performed with platinum crucibles in an atmosphere of flowing air or Ar/H_2 (7%) at a heating rate of 10 °C/min.

A JEOL 5800 scanning electron microscope (Tokyo, Japan) equipped with a Tracor-Northern energy-dispersive system (EDS, Middleton, WI, USA) was used for the overall microstructural analysis.

The surfaces of the TiO_2, the non-stoichiometric TiO_{2-x} and the Ti_2O_3 ceramics were analysed using X-ray photoelectron spectroscopy (TFA XPS spectrometer, Physical Electronics, Chanhassen, MN, USA). All the spectra were recorded using monochromated Al Kα (1486.8 eV). Two types of spectra were recorded: wide-energy survey scans and high-energy-resolution narrow scans of the Ti 2p, O 1s and C 1s spectral regions with an energy resolution of 0.6 eV. The energy scale of the spectra was corrected using the binding energy of the carbon C 1s peak at 284.6 eV. Regions of 400 μm in diameter and a depth of 1–3 nm were analysed. The surface composition was calculated from the XPS intensities using the relative sensitivity factors provided by the instrument manufacturer.[23]

The contact-angle measurements were performed on the as-sintered ceramic surfaces. After the sintering process the pellets were removed from the furnace and put directly into a desiccator. The contact angle was measured for several samples and the reported value is an average of these measurements. A Fibro DAT 1100 Dynamic Contact Angle and Absorption Tester (Fibro Systems AB, Stockholm, Sweden) was used for the measurements. The volume of the water droplet was 4 μl.

3. Results and discussion

At room temperature TiO_2 powder is white and crystallises in the tetragonal rutile structure with calculated lattice parameters of $a = 0.45902 \pm 0.00007$ nm and $c = 0.29580 \pm 0.00007$ nm. The non-stoichiometric TiO_2 powder (denoted TiO_{2-x}) obtained after firing the TiO_2 at 1400 °C in Ar/H_2 (7%) was dark blue. It crystallises in the tetragonal rutile structure with lattice parameters of $a = 0.4588 \pm 0.0007$ nm and $c = 0.2957 \pm 0.0001$ nm. An SEM image of the TiO_{2-x} powder and its XRD pattern are shown in Fig. 2.

Commercially available Ti_2O_3 powder is very coarse, with a particle size up to 44 μm. An SEM image of some Ti_2O_3 powder that was high-energy milled for 12 h is shown in Fig. 3a. With this technique the particle size of the Ti_2O_3 was reduced to a median grain size of 2 μm. The X-ray powder-diffraction analysis of the as-received Ti_2O_3 powder shows that the Ti_2O_3 phase coexists with a small amount of Ti_3O_5 phase (PDF 72-519[22],

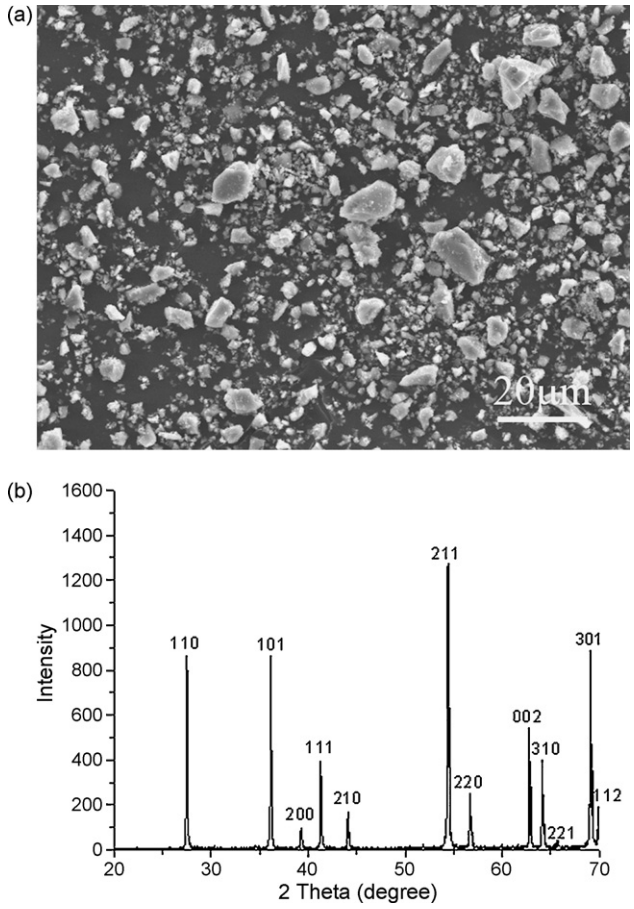

Fig. 2. (a) SEM image of TiO_{2-x} powder and (b) X-ray powder-diffraction pattern of TiO_{2-x} powder.

Fig. 3b). Ti_2O_3 crystallizes in a rhombohedral crystal structure with $a = 0.54314 \pm 0.00006$ nm and $\alpha = 56.659 \pm 0.005°$.

The TG curves of the TiO_2 in air and in Ar/H_2 (7%) are shown in Fig. 4. The mass changes of the micrometer-sized TiO_2 in air and in Ar/H_2 (7%) at 1400 °C are 0.41% and 1.14%, respectively.

The sintering curves for the TiO_2 in air, for the TiO_2 in Ar/H_2 (7%), and for the as-received and high-energy-milled Ti_2O_3 in Ar/H_2 (7%) up to 1400 °C are shown in Fig. 5. The onset temperature for the TiO_2 in air and in Ar/H_2 (7%) was 1000 °C. The densification process was incomplete up to 1400 °C, which is evident from the shapes of the curves. The TiO_2 in air shrank by 21% at 1360 °C and in Ar/H_2 (7%) it shrank by 17% at 1400 °C. The as-received Ti_2O_3 powder did not exhibit any shrinkage up to 1400 °C, while the onset temperature for the high-energy-milled Ti_2O_3 was 1200 °C. Since the chemical composition of the as-received and high-energy-milled Ti_2O_3 is identical, it seems reasonable to suppose that the different sintering behaviours are a result of the dissimilar particle sizes of the powders. The high-energy-milled Ti_2O_3 powder with a particle size of 2 μm started to densify at lower temperatures than the as-received Ti_2O_3 powder with 40 μm particles. This influence of the particle size on the densification process is well known, and our observations are in agreement with those reported in the literature.[24]

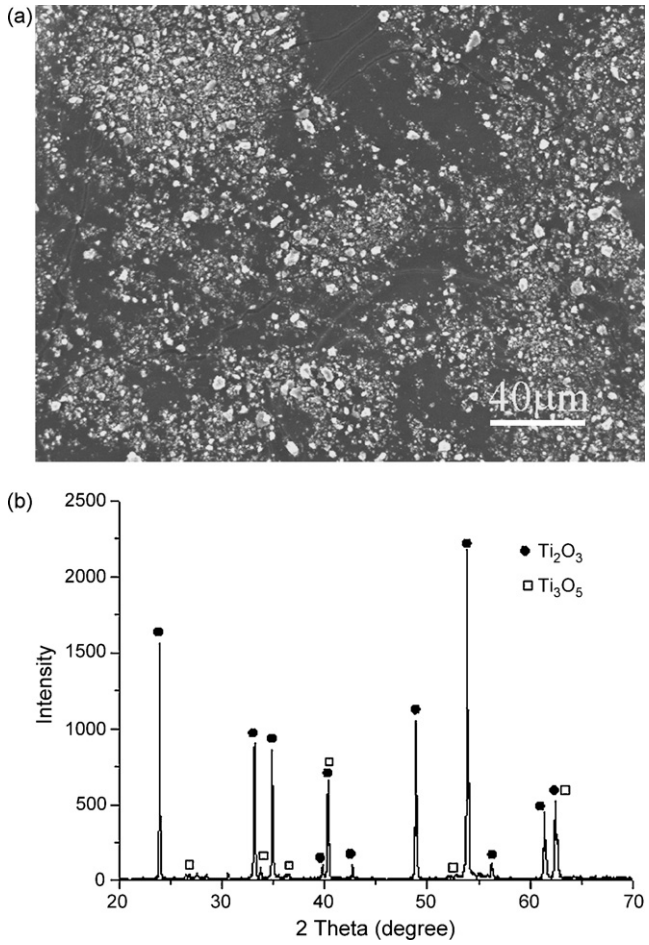

Fig. 3. (a) SEM image of high-energy-milled Ti_2O_3 powder and (b) X-ray powder-diffraction pattern of as-received Ti_2O_3 powder.

SEM images of a cross-section of the TiO_2 pellet and its surface sintered at 1400 °C for 2 h in air are shown in Fig. 6. The sintered TiO_2 is dense, albeit with some pores. The surface of the TiO_2 is dense with clearly observable grains of up to 50 μm in diameter (Fig. 6b). The XRD analysis of theTiO_2 ceramic shows that it crystallise in the rutile tetragonal structure with calculated lattice parameters of $a = 0.45902(7)$ nm and $c = 0.29580(7)$ nm.

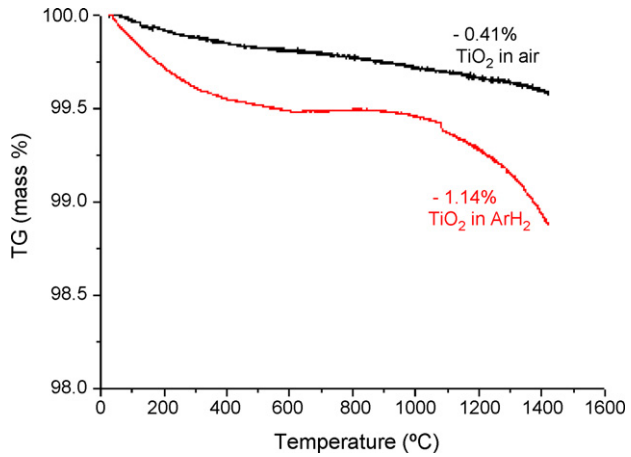

Fig. 4. TG curves of TiO_2 in air and in Ar/H_2 (7%) up to 1400 °C.

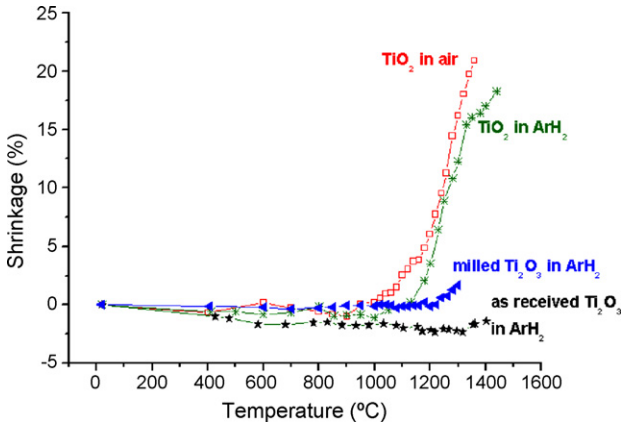

Fig. 5. Sintering curves for TiO_2 in air, TiO_{2-x} in Ar/H_2 (7%), as-received Ti_2O_3 in Ar/H_2 (7%) and high-energy-milled Ti_2O_3 in Ar/H_2 (7%) from room temperature to 1400 °C.

SEM images of the non-stoichiometric TiO_{2-x} ceramic and its surface sintered at 1400 °C for 2 h in Ar/H_2 (7%) are shown in Fig. 7a and b, respectively. The microstructure of the ceramic consists of a matrix phase, where only titanium was detected by the SEM/EDS analysis. From the SEM images it is clear that the non-stoichiometric TiO_{2-x} is more porous than the TiO_2 ceramic sintered in air. This is consistent with the results of the sintering behaviour of the TiO_2 in air and in Ar/H_2 (Fig. 5).

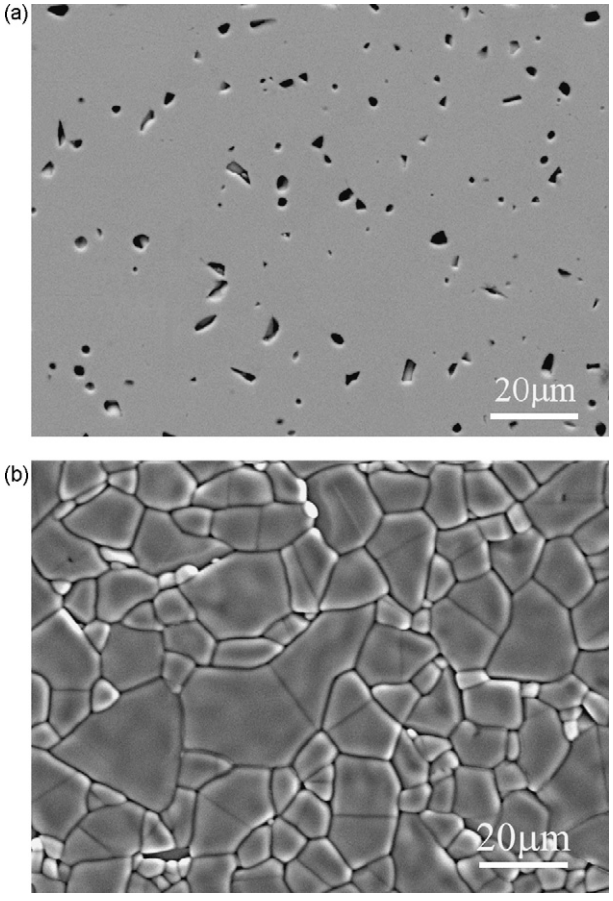

Fig. 6. SEM image of TiO_2 sintered at 1400 °C for 2 h in air: (a) polished cross-section of TiO_2 and (b) surface of TiO_2.

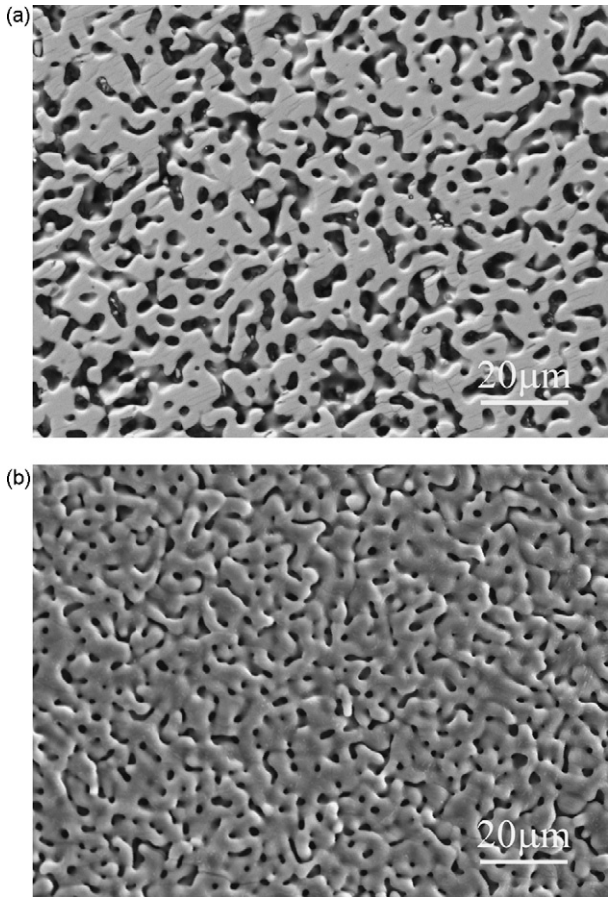

Fig. 7. SEM image of TiO_{2-x} sintered at 1400 °C for 2 h in Ar/H_2 (7%) atmosphere: (a) polished cross-section of TiO_{2-x} and (b) surface of TiO_{2-x}.

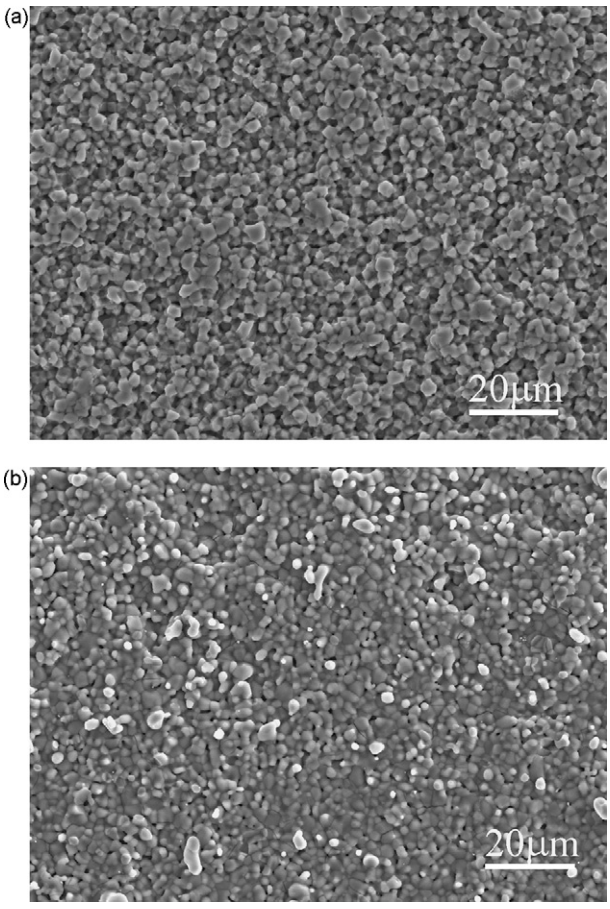

Fig. 9. SEM image of Ti_2O_3/Ti_3O_5 sintered at 1400 °C for 2 h in Ar/H_2: (a) polished cross-section of Ti_2O_3/Ti_3O_5 and (b) surface of Ti_2O_3/Ti_3O_5.

The high-energy-milled Ti_2O_3 powder was sintered at 1400 °C for 2 h in Ar/H_2 (7%) (denoted Ti_2O_3). The XRD spectrum of the Ti_2O_3 ceramic is shown in Fig. 8. All the diffraction peaks were identified as the Ti_2O_3 (PDF 10-0063)[22] or Ti_3O_5 (PDF 72-0519)[22] phases. SEM images of the cross-section and the surface of the sintered Ti_2O_3 ceramic are shown in Fig. 9. From these results it is evident that the Ti_3O_5 phase is formed during the sintering of Ti_2O_3. For that reason, Ti_2O_3 sintered under these experimental conditions will be subsequently referred to as Ti_2O_3/Ti_3O_5.

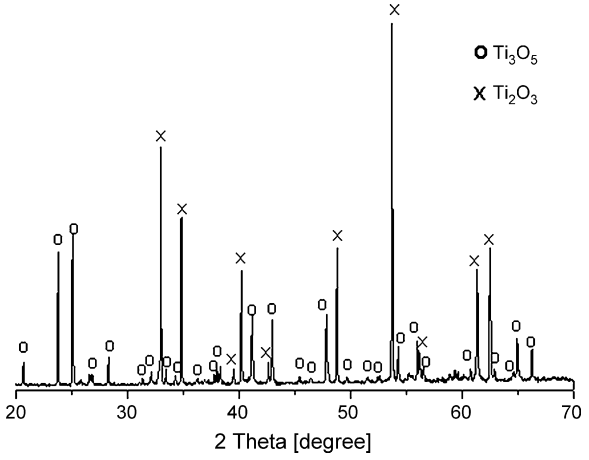

Fig. 8. XRD spectrum of Ti_2O_3/Ti_3O_5 sintered at 1400 °C for 2 h in Ar/H_2 (7%).

The main problem when sintering Ti_2O_3 powder is to ensure a highly reducing atmosphere in the furnace. Just a trace of oxygen present during the high-temperature processing of Ti_2O_3 is sufficient to cause Ti^{3+}–Ti^{4+} oxidation, and as a consequence the formation of Ti_2O_{2n-1} phases. The sintering conditions – atmosphere, temperature and time – have to be optimised and controlled very carefully in order to produce a ceramic with reproducible properties.

The contact angles for water on the as-sintered surface of TiO_2 fired at 1400 °C in air, the non-stoichiometric TiO_{2-x} sintered at 1400 °C in Ar/H_2 (7%), and the Ti_2O_3/Ti_3O_5 sintered at 1400 °C in Ar/H_2 (7%) are shown in Table 1. All the examined pellets show a hydrophilic surface. A contact angle of $67 \pm 2°$ was measured on the TiO_2's surface, which is in accordance with reference.[18] The contact angles on the TiO_{2-x} and

Table 1
Contact angles of ceramics in the Ti–O system

	Contact angle (°)	Identified phases by XRD
TiO_2	67	TiO_2—rutile
TiO_{2-x}	26	TiO_2—rutile
Ti_2O_3/Ti_3O_5	18	Ti_2O_3, Ti_3O_5

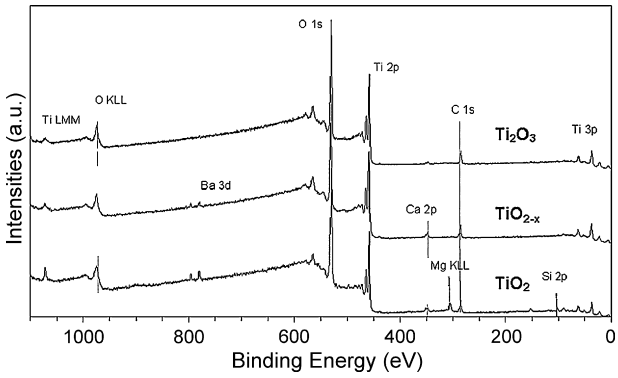

Fig. 10. XPS survey spectra from TiO_2, non-stoichiometric TiO_{2-x} and Ti_2O_3/Ti_3O_5 pellet surfaces.

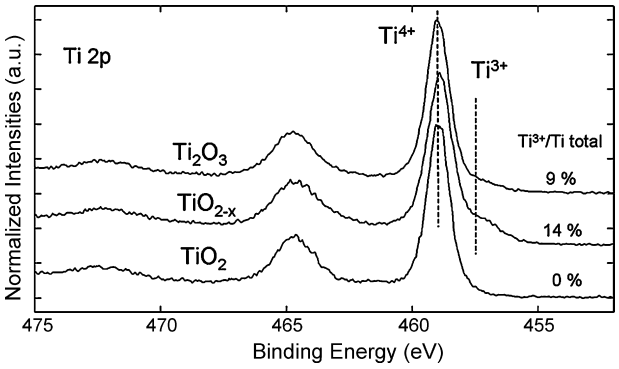

Fig. 11. High-energy-resolution XPS spectra of Ti 2p from TiO_2, TiO_{2-x} and Ti_2O_3/Ti_3O_5.

Ti_2O_3/Ti_3O_5's surfaces were considerably lower, i.e., $26 \pm 5^\circ$ and $18 \pm 5^\circ$.

The authors are aware that there are numerous problems associated with measuring the water-contact angle on TiO_2 surfaces. The surface of TiO_2 is a high-energy one and therefore organic contaminants are easily accumulated on it. Under UV irradiation these contaminants may decompose, and so the surface will become more hydrophilic simply because it may be cleaner. However, Stevens et al.[17] confirmed the hydrophobic-to-hydrophilic transition of TiO_2 as a result of light irradiation. The results presented here address the water-contact angle measured on non-illuminated and as-sintered TiO_2, TiO_{2-x} and Ti_2O_3 ceramic samples that were handled identically after the thermal treatment, i.e., they were removed from the furnace and put immediately into the desiccator. The surface roughness is also a factor that may decrease the water-contact angle. According to the Wenzel equation, a lower contact angle should be observed on a rough surface than on a smooth one.[17] However, the calculation shows that the decrease in the water-contact angle from 67° for TiO_2 to 26° for non-stoichiometric TiO_{2-x} cannot only be a consequence of the surface roughness. The water-contact angle on a rough surface (θ) can be calculated as $\cos\theta = r\cos\theta_o$, where r is the roughness factor and θ_o is the water-contact angle on a flat surface. Taking into consideration the roughness factor (r), which is reported to be 1.39 for 0.5-μm TiO_2 particles,[17] and the water-contact angle θ_o of 67° for TiO_2, then the water-contact angle on TiO_{2-x}, due only to the roughness difference, should have a value of 57°. This calculation shows that the decrease in the contact angle on the TiO_{2-x} is certainly not just a consequence of the surface roughness; it has to be associated with the different chemical composition of the surface, i.e., the formation of Ti^{3+}, which was also identified using XPS analyses.

Fig. 10 shows typical X-ray photoelectron spectroscopy (XPS) survey spectra of the ceramic pellets, i.e., TiO_2 sintered at 1400 °C in air, non-stoichiometric TiO_{2-x} sintered at 1400 °C in Ar/H_2, and Ti_2O_3 sintered at 1400 °C in Ar/H_2, i.e., Ti_2O_3/Ti_3O_5. Ti, O and C were detected at the surface for all the samples, as were traces of Ca. Traces of Ba were detected in the non-stoichiometric TiO_{2-x} sample; traces of Ba and Mg were detected in the mechanically activated Ti_2O_3/Ti_3O_5 sample; and traces of Si, Mg and Ba were detected on the TiO_2's surface. We suppose that these additional peaks with low intensity observed at the surface are a consequence of the presence of traces of these oxides in the raw materials. The chemical compositions of the ceramic surfaces were calculated from the XPS spectra and are presented in Table 2. It should be noted that the presence of impurities at the TiO_2, TiO_{2-x} and Ti_2O_3 ceramic interfaces can influence the absolute values of the water-contact angles however there is also a clear tendency for a decrease in the water-contact angles for the TiO_{2-x} and Ti_2O_3 compared to the TiO_2.

High-energy-resolution XPS spectra for Ti 2p are shown in Fig. 11. Using a curve-fitting technique they were decomposed into two doublets associated with the Ti^{4+} and Ti^{3+} valence states at binding energies of 458.3 and 456.3 eV, respectively, according to the literature.[25] The relative intensities of the Ti^{3+} and Ti^{4+} components were calculated. The TiO_2 ceramic contains only the Ti^{4+} component at the surface. However, at the non-stoichiometric TiO_{2-x} ceramic surface, obtained by sintering TiO_{2-x} powder in Ar/H_2 (7%), 14% of the Ti atoms were found to be in the Ti^{3+} valence state. A total of 9% of the Ti atoms are in the Ti^{3+} valence state at the Ti_2O_3/Ti_3O_5 surface sintered at 1400 °C in Ar/H_2 (7%). In addition, we observed that the O/Ti ratio changes at the surface of the sample. The highest ratio was obtained with the TiO_2 sample, i.e., 3.6, while a value of 2.3 was observed for both the non-stoichiometric TiO_{2-x} and the

Table 2
Chemical composition (at.%) of TiO_2, non-stoichiometric TiO_{2-x} and Ti_2O_3/Ti_3O_5 pellet surface, determined by XPS analysis

	Ti	O	C	Ca	Si	Mg	Ba	N	O/Ti	Ti^{3+}/total Ti
TiO_2	16.5	60.2	13.4	1.3	3.4	4.8	0.4	0	3.6	0
TiO_{2-x}	24.4	56.8	17.1	1.5	0	0	0.2	0	2.3	14
Ti_2O_3	24.8	56.4	18.2	0.6				0	2.3	9

high-energy-milled Ti_2O_3/Ti_3O_5. This means that the surface oxygen concentrations on the non-stoichiometric TiO_{2-x} and the high-energy-milled Ti_2O_3/Ti_3O_5 are lower than on the TiO_2 due to oxygen vacancies. The O/Ti ratios for all three measured samples are higher than were expected (∼2). This may be due to the quantification procedure or the adsorption of oxygen-based species from the air onto the surface during the manipulation of the samples.

Based on the XPS results, the contact-angle measurements and the structural analyses it follows that the surface properties of ceramics in the Ti–O system are related to the valence state of the titanium ions. The formation of Ti^{3+} at the surface results in a decrease of the oxygen/titanium ratio and a decrease in the water-contact angles.

Our results indicate that the wettability of ceramics in the Ti–O system can be modified not only by light irradiation, as was described in the literature, but also by changing the valence state of the titanium ions during the processing. This can be achieved by choosing the appropriate atmosphere during the thermal treatment.[17,18] When TiO_2 was sintered in air it crystallised in the tetragonal rutil structure. The ceramic was white and with a dense microstructure (Fig. 6). XPS results show that only Ti^{4+} ions are present at the surface. Since no Ti^{3+} was detected at the TiO_2 surface, the formation of oxygen vacancies was not expected. Based on these observations we suppose that the TiO_2 surface has a high water-contact angle. Indeed, the measured water-contact angle of $67 \pm 2^\circ$ agrees well with the published data for a non-exposed TiO_2 surface.[17,18]

Also, TiO_{2-x} sintered in Ar/H_2 (7%) crystallises in the tetragonal rutil crystal structure; however, after the sintering it becomes dark blue. This is an indication that the valence state of the titanium is changed. Actually, for both the non-stoichiometric TiO_{2-x} and Ti_2O_3/Ti_3O_5 surfaces Ti^{3+} states were detected by XPS analyses. In order to achieve electroneutral conditions in the non-stoichiometric TiO_{2-x}, in addition to Ti^{3+} the formation of oxygen vacancies is expected. As reported in the literature,[4,5] the water molecules can be easily incorporated at an oxygen-vacancy-containing surface and the wettability of the surface should increase. Our measurements confirm the correlation between the Ti^{3+} and the water-contact angle. The water-contact angles of the non-stoichiometric TiO_{2-x} and Ti_2O_3/Ti_3O_5 are lower than that of the TiO_2, i.e., $26 \pm 5^\circ$, $18 \pm 5^\circ$ and $67 \pm 2^\circ$, respectively.

4. Summary

We have shown for the first time that the water-contact angle of ceramics in the Ti–O system can be modified, not only by irradiating the TiO_2 with light of a specific wavelength, but also by a partial reduction of Ti^{4+} to Ti^{3+} using a lower oxygen partial pressure during the sintering process. The introduction of Ti^{3+} into the stoichiometric TiO_2 rutile structure significantly improves the wettability of the as-sintered ceramics.

TiO_2, non-stoichiometric TiO_{2-x} and Ti_2O_3/Ti_3O_5 ceramics with various Ti^{3+}/Ti^{4+} ratios were prepared from TiO_2 and Ti_2O_3 powder by sintering them at 1400 °C in air and in Ar/H_2 (7%). Dense TiO_2 with only Ti^{4+} at the interface was prepared by sintering the TiO_2 powder in air; however, Ti^{3+} is introduced at the interface of ceramics in the Ti–O system when the powder is sintered in Ar/H_2 (7%). The formation of Ti_2O_3 together with Ti_3O_5 was observed when Ti_2O_3 was sintered in Ar/H_2 (7%). Totals of 14% and 9% of Ti^{3+} were measured at the non-stoichiometric TiO_{2-x} and Ti_2O_3/Ti_3O_5 interfaces. The water-contact angle for TiO_2 was $67 \pm 2^\circ$ and this value decreased significantly when Ti^{3+} was present at the interface. The water-contact angle was $26 \pm 5^\circ$ for the non-stoichiometric TiO_{2-x} and $18 \pm 5^\circ$ for the Ti_2O_3/Ti_3O_5.

Acknowledgements

This research was supported by the project EZPLATE No. 030 898. Dr. Janez Holc is acknowledged for valuable discussions.

References

1. Linsebigler, A. L., Lu, G. and Yates, J. T., Photocatalysis on TiO_2 surfaces: principles, mechanisms, and selected results. *Chem. Rev.*, 1995, **95**, 735–758.
2. Rothschild, A., Edelman, F., Komem, Y. and Cosandey, F., Sensing behavior of TiO_2 thin films exposed to air at low temperatures. *Sens. Actuator B*, 2000, **67**, 282–289.
3. Takeuchi, K., Nakamura, I., Matsumoto, O., Sugihara, S., Ando, M. and Ihara, T., Preparation of visible-light-responsive titanium oxide photocatalysts by plasma treatment. *Chem. Lett.*, 2000, **29**(12), 1354–1355.
4. Fujishima, A., Rao, T. N. and Tryk, D. A., Titanium dioxide photocatalysis. *J. Photochem. Photobiol. C: Photochem. Rev.*, 2000, **1**, 1–21.
5. Carp, O., Huisman, C. L. and Reller, A., Photoinduced reactivity of titania dioxide. *Prog. Solid State Chem.*, 2004, **32**, 33–177.
6. Legrini, O., Oliveros, E. and Brown, A. M., Photochemical processes for water treatment. *Chem. Rev.*, 1993, **93**, 671–698.
7. Herrmann, J. M., Heterogeneous photocatalysis: fundamentals and applications to the removal of various types of aqueous pollutants. *Catal. Today*, 1999, **53**, 115–129.
8. Samsonov, G. V., *The Oxide Handbook*. IFI Plenum, New York, 1982.
9. Grant, F. A., Properties of rutile. *Rev. Modern Phys.*, 1959, **32**, 646–674.
10. Baur, W. H., Über die verfeinerung der kristallstrukturbestimmung einiger vertreter des rutiltyps: TiO_2, SnO_2, GeO_2 und MgF_2. *Acta Cryst.*, 1956, **9**, 515–520.
11. Diebold, U., The surface science of titania dioxide. *Surf. Sci. Rep.*, 2003, **48**, 53–229.
12. Millot, F., Blanchin, M.-G., Tetot, R., Marucco, J.-F., Poumellec, B., Picard, C. and Touzelin, B., High temperature nonstoichiometric rutile TiO_{2-x}. *Prog. Solid State Chem.*, 1987, **17**, 263–293.
13. Marucco, J. F., Gautron, S. and Lemasson, P., Thermogravimetric and electrical study on non-stoichiometric titanium oxide TiO_{2-x} between 800 and 1100 °C. *J. Phys. Chem. Solids*, 1981, **42**, 363–367.
14. Bursill, L. A. and Hyde, B. G., Crystallographic shear in the higher titanium oxides: structure, texture, mechanisms and thermodynamics. *Prog. Solid State Chem.*, 1972, **7**, 177–253.
15. Robinson, W. R., The crystal structure of Ti_2O_3, a semiconductor and $(Ti_{0.900}V_{0.100})_2O_3$, a semimetal. *J. Solid State Chem.*, 1974, **9**, 255–260.
16. Rammamorthy, M., Vanderbilt, D. and King Smith, R. D., First-principles calculations of the energetics of stoichiometric TiO_2 surfaces. *Phys. Rev. B*, 1994, **49**, 16721–16727.
17. Stevens, N., Priest, C. I., Sedev, R. and Ralston, J., Wettability of photoresponsive titanium dioxide surfaces. *Langmuir*, 2003, **19**, 3272–3275.
18. Wang, R., Hashimoto, K., Fujishima, A., Chikuni, M., Kojima, E., Kitamura, A., Shimohigoshi, M. and Watanabe, T., Light-induced amphilic surfaces. *Nature*, 1997, **388**, 431–432.

19. Tosatti, S., Mitchel, R., Textor, M. and Spencer, N. D., Self-assembled monolayers of dodecyl and hydroxy-dodecyl phosphates on both smooth and rough titanium and titanium oxide surfaces. *Langmuir*, 2002, **18**, 3537–3548.
20. Takeda, S., Fukawa, M., Hayashi, Y. and Matsumoto, K., Surface OH group governing adsorption properties of metal oxide films. *Thin Solid Films*, 1999, **339**, 220–224.
21. Kuscer, D., Meden, A., Holc, J. and Kosec, M., The mechano-synthesis of lead–magnesium–niobate ceramics. *J. Am. Ceram. Soc.*, 2006, **89**(10), 3081–3088.
22. PDF-ICDD, *PCPDFWin Version 2.2, June 2001*. International Centre for Diffraction Data, 2002.
23. Moulder, J. F., Stickle, W. F., Sobol, P. E. and Bomben, K. D., *Handbook of X-Ray Photoelectron Spectroscopy*. Physical Electronics Inc., Eden Prairie, Minnesota, USA, 1995.
24. Reed, J. S., *Principle of Ceramic Processing* (*2nd ed.*). John Wiley & Sons, 1995, p. 595.
25. Mayer, J. T., Diebold, U., Madey, T. E. and Garfunkel, E., Titanium and reduced titania overlayers on titanium dioxide (1 1 0). *J. Electr. Spectrosc. Relat. Phenom.*, 1995, **73**, 1–11.